

Atomic Layer Deposition of Y_2O_3 Thin Films from Yttrium Tris(N,N' -diisopropylacetamidate) and Water

Philippe de Rouffignac,[†] Jin-Seong Park,[†] and Roy G. Gordon*

Department of Chemistry and Chemical Biology, Harvard University, Cambridge, Massachusetts 02138

Received March 22, 2005. Revised Manuscript Received May 20, 2005

Y_2O_3 thin film was deposited by atomic layer deposition (ALD) with a new precursor yttrium tris(N,N' -diisopropylacetamidate), $Y(\text{Pr}_2\text{amd})_3$, and water. The precursor was thermally stable and volatile and had high reactivity with water. The growth rate of Y_2O_3 films was $0.8 \text{ \AA}/\text{cycle}$ over a wide temperature range ($150\text{--}280 \text{ }^\circ\text{C}$). The films were very pure ($C, N < 0.5 \text{ at. } \%$) and had a refractive index of 1.8. The films were smooth and had a cubic polycrystalline structure. High quality films were also deposited in 40:1 aspect ratio profiled substrates. Y_2O_3 films adsorbed water after air exposure because Rutherford backscattering spectroscopy (RBS) and X-ray photoelectron spectroscopy (XPS) showed an increased oxygen ratio ($O/Y > 1.5$) and $-\text{OH}$ bonds in air-exposed films. A relatively high permittivity (~ 12), a low leakage current density ($< 10^{-7} \text{ cm}^2$ at 2 MV/cm) and high electrical breakdown field ($\sim 5 \text{ MV/cm}$) were measured for capacitors prepared from Al_2O_3 (10 \AA)/ Y_2O_3 /n-Si structures. Uncapped Y_2O_3 films showed flatband voltage shifts of 1 V and increased leakage current prior to annealing. ALD Y_2O_3 is a promising dielectric for advanced electronic applications in nanoscale devices.

Introduction

Yttrium oxide (Y_2O_3) is a very interesting material for potential applications because of its relatively high permittivity ($10\text{--}17$),¹ high melting point ($\sim 2439 \text{ }^\circ\text{C}$), a relatively large band gap energy ($\sim 5.5 \text{ eV}$), and a refractive index of 1.8.² In microelectronics, Y_2O_3 is a candidate to be a gate dielectric material (such as Al_2O_3 , HfO_2 , ZrO_2 , La_2O_3 , Pr_2O_3 , and Gd_2O_3 , among others)^{3–5} which would require a high permittivity (> 10), compatibility with silicon, good thermal stability, and a relatively large conduction band offset and valence band offset (2.3 and 2.2 eV, respectively, for Y_2O_3).⁶ Therefore Y_2O_3 could be considered for a replacement of SiO_2 in transistors and memories. In addition, Y_2O_3 could be used as a waveguide material due to its high refractive index, or as a buffer layer for ferroelectrics and superconductors because of its low lattice-mismatch with silicon. Y_2O_3 has also been investigated for use as optical² and protective coating layers⁷ due to a high melting point and refractive index. In addition, Y_2O_3 is a constituent of several more complex thin film materials. $\text{YBa}_2\text{Cu}_3\text{O}_{7-\delta}$ ⁸ is a well-known high- T_c superconductor, and many studies of yttrium-stabilized ZrO_2 ⁹ and $Y_2O_3:\text{Eu}^{2+}$ have been published.¹⁰

Y_2O_3 thin films have been deposited by many methods, including electron-beam evaporation,¹¹ laser ablation, sputtering,^{12,13} thermal oxidation,¹⁴ vacuum thermal evaporation,¹⁵ molecular-beam epitaxy,¹⁶ metal–organic chemical vapor deposition (CVD),¹⁷ low-pressure CVD,¹⁸ and atomic layer deposition (ALD).^{19–21} ALD is a method in which a thin film is deposited by supplying saturating pulses of precursor vapors sequentially. The precursor vapor distributes on a nonuniform surface until the surface is saturated (self-limiting mechanism). The subsequent precursor vapor reacts with the chemisorbed precursor on the surface. ALD presents several advantages such as superior step coverage, excellent film uniformity over large areas, and exact thickness control at the nanoscale, good surface morphologies, and low film impurities.²²

* To whom correspondence should be addressed. E-mail: gordon@chemistry.harvard.edu.

[†] These authors contributed equally to this work.

- (1) Wilk, G. D.; Wallace, R. M.; Anthony, J. M. *J. Appl. Phys.* **2001**, *89*, 5243.
- (2) Atanassov, G.; Thielsch, R.; Popov, D. *Thin Solid Films* **1993**, *223*, 228.
- (3) Hu, H.; Zhu, C.; Lu, Y. F.; Li, M. F.; Cho, B. J. *IEEE Electron Device Lett.* **2002**, *23*, 514.
- (4) Chen, S. B.; Lai, C. H.; Chin, A. *IEEE Electron Device Lett.* **2002**, *23*, 185.
- (5) Leskella, M.; Ritala, M. *J. Solid State Chem.* **2003**, *171*, 170.
- (6) Robertson, J. *J. Vac. Sci. Technol. B* **2000**, *18*, 1785.
- (7) Bonnet, G.; Lachkar, M.; Larpin, J. P.; Colson, J. C. *Solid State Ionics* **1994**, *72*, 344.
- (8) Klippe, L.; Wahl, G. *J. Alloys Compd.* **1997**, *251*, 249.

- (9) Dubordieu, C.; Kang, S. B.; Li, Y. Q.; Kulesha, G.; Gallois, B. *Thin Solid Films* **1999**, *229*, 165.
- (10) McKittrick, J.; Hirata, G. A.; Bacalski, C. F.; Sze, R.; Mourant, J.; Hubbard, K. M.; Pattilo, S.; Salazar, K. V.; Trkula, M.; Gosnell, T. R. *J. Mater. Res.* **1998**, *13*, 3019.
- (11) Fukumoto, H.; Imura, T.; Osaka, Y. *Appl. Phys. Lett.* **1987**, *51*, 919.
- (12) Araiza, J. J.; Cardenas, M.; Falcony, C.; Mendez-Garcia, V. M.; Lopez, M.; Contreras-Puente, G. *J. Vac. Sci. Technol. A* **1998**, *16*, 3305.
- (13) Horng, R. H.; Wu, D. S.; Yu, J. W.; Kung, C. Y. *Thin Solid Films* **1998**, *289*, 234.
- (14) Gurvitch, M.; Manchanda, L.; Gibson, J. M. *Appl. Phys. Lett.* **1987**, *51*, 919.
- (15) Bezuidenhout, D. F.; Pretorius, R. *Thin Solid Films* **1986**, *139*, 121.
- (16) Vyas, J. C.; Kothiyal, G. P.; Muthe, K. P.; Gandhi, D. P.; Debnath, A. K.; Sabharwal, S. C.; Gupta, M. K. *J. Cryst. Growth* **1993**, *130*, 59.
- (17) Varhue, W. J.; Massimo, M.; Carrulli, J. M.; Baranauskas, V.; Adams, E.; Broitman, E. *J. Vac. Sci. Technol. A* **1993**, *11*, 1870.
- (18) Sharma, R. N.; Rastogi, A. C. *J. Appl. Phys.* **1994**, *76*, 4215.
- (19) Molsa, H.; Niinistö, L.; Utrianinen, M. *Adv. Mater. Opt. Electron.* **1997**, *4*, 389.
- (20) Putkonen, M.; Sajavaara, T.; Johansson, L.; Niinistö, L. *Chem. Vap. Dep.* **2001**, *7*, 44.
- (21) Niinistö, J.; Putkonen, M.; Niinistö, L. *Chem. Mater.* **2004**, *16*, 2953.
- (22) Ritala, M.; Leskela, M. In *Handbook of Thin Film Materials*; Nalwa, H. S., Ed.; Academic Press: San Diego, 2001; Vol 1, pp 103–159.

In a previously published ALD process for Y_2O_3 ,²⁰ $Y(thd)_3$, $Y(thd)_3(bipy)$, and $Y(thd)_3(phen)$ were used as metal precursors with ozone as the oxygen source. This results in a low growth rate (0.23 Å/cycle) within the deposition temperature ranges (250–375 °C) and the impurity levels such as hydrogen and carbon are high (around 6 at. % C and 10 at. % H depending on deposition temperature), while some nitrogen (0.2–0.3 at. %) is observed in the films below 325 °C. Generally a highly reactive oxygen source, such as ozone, may dissociate the ligand from the precursor in such a way that some carbon and nitrogen remain in the film. Ozone has been known to further oxidize the Si to SiO_x at the interface thereby reducing the overall dielectric constant of the stack. Other precursors that have been used are based on the cyclopentadienyl-type yttrium compounds. In particular $(CH_3Cp)_3Y$ and Cp_3Y ($Cp=C_5H_5$) have been investigated using water as the oxygen source.²¹ The films show high growth rate (1.2–1.8 Å/cycle) as a function of deposition temperature but have very poor electronic properties such as a slightly lower permittivity (~ 10), a very strong negative shift of the flat band voltage (~ 5 V), high leakage current (10^{-5} A/cm² at 1.5 MV/cm) and a low breakdown field (1.2–1.6 MV/cm).

In this study, we developed a new yttrium precursor which is volatile and thermally stable and has good reactivity with water. The deposited Y_2O_3 films show a high growth rate, smooth surface, and excellent electrical properties.

Experimental Section

Y_2O_3 thin films were deposited with a horizontal gas flow type reactor²³ using yttrium tris(*N,N'*-diisopropylacetamidate) $Y(Pr_2amd)_3$ and water. The deposition temperature was varied from 150 to 270 °C and the pressure was set to 0.3 Torr using high-purity nitrogen as the carrier gas. The yttrium precursor and water were kept at 130 and 25 °C, respectively.

Film thickness and refractive index were determined with a Rudolph Research Auto El-II ellipsometer at a wavelength of 632.8 nm with the incident angle set at 70°. Rutherford backscattering spectroscopy (RBS) (General Ionics model 4117, 1.7 MeV Tandemtron) and X-ray photoelectron spectroscopy (XPS) (Surface Science Lab S5X-100) were used to analyze the composition and binding structure of the yttrium oxide films. Films were deposited on glassy carbon substrates (Alpha Aesar, type 2) for RBS measurements. TG measurements were made using a TA Instruments TGA Q50 at atmospheric pressure in a dry nitrogen glovebox. X-ray diffraction using a Scintag model XDS 2000 with copper $K\alpha$ radiation (1.54 nm wavelength) was carried out to measure crystallinity. A DI Nanoscope III AFM was used in the tapping mode to examine surface roughness. Electrical properties ($I-V$ and $C-V$) were measured on Pt/ $Al_2O_3/Y_2O_3/n$ -type Si (5–10 Ωcm) MOS (metal–oxide–semiconductor) structures using a Signatone probe station, an HP 4275a LCR meter, and a Keithley 2400 source meter. The dot size was 1.05×10^{-3} cm² as determined by a FEI dualbeam field emission SEM and using a standard SiO_2 sample. After deposition of the film, the backs of the substrates were treated with a 10% HF solution for 30 s to remove Y_2O_3 and SiO_2 . Pt was sputtered onto the bare Si to form the back contact.

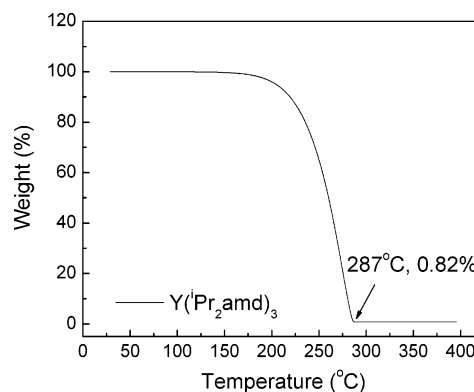


Figure 1. TG plot of the yttrium precursor.

Results and Discussion

Synthesis of $Y(Pr_2amd)_3$. The yttrium precursor was synthesized by the reaction of YCl_3 and lithium *N,N'*-diisopropylacetamidate by the following steps carried out under a dry nitrogen atmosphere. A solution of methyl lithium (1.6 M in ether) was added dropwise to an equivalent amount of 1,3-diisopropylcarbodiimide (0.55 M in ether) at -30 °C. The mixture was allowed to warm to room temperature and stirred for 4 h. Three equivalents of the resulting solution of lithium *N,N'*-diisopropylacetamidate was mixed with a slurry of YCl_3 (1 equiv) in tetrahydrofuran. The suspension was stirred overnight (12 h) at room temperature. The gray suspension was filtered through Celite to remove the solid LiCl salt. The transparent solution was dried under vacuum leaving a white solid. This white solid was purified using sublimation. During the course of the sublimation two different compounds were isolated. A white solid was obtained from the crude material during the initial sublimation. This material had a high volatility (50 mTorr at 70 °C), and was determined to be an organic byproduct from a side-reaction. The second compound that sublimed from the crude material was found by NMR (C_6D_6 δ 3.16[$CH(CH_3)_2$]; 1.72-[CH_3]; 1.227[$CH(CH_3)_2$]) to be the desired product $Y(Pr_2amd)_3$. This yttrium precursor is pale blue and sublimates with a pressure of 30 mTorr at 90 °C. The melting point of this precursor could not be detected below 220 °C. Thermogravimetric (TG) analysis (Figure 1) shows that the compound has a very clean single-step sublimation and leaves residue of less than 1% by mass. An isothermal TG done at the temperature the precursor was used (130 °C) displayed a constant sublimation rate of $0.18 \mu\text{g}/\text{sec}\cdot\text{cm}^2$ and showed almost no residue, indicating that this compound is thermally stable during sublimation.

ALD of Y_2O_3 Thin Films. The yttrium oxide films were deposited on HF etched n-type silicon at 280 °C. The precursor dose was controlled by the volume of vapor that is trapped and released into the chamber for each cycle. The vapor volumes of yttrium precursor and water were 120 and 20 cm³, respectively. Figure 2 shows the thickness per cycle as a function of the yttrium precursor dose. The precursor vapor spaces were opened to the reaction chamber for 1 s with a 10-s purge for the yttrium precursor and a 60-s purge for the H_2O . As can be seen from the saturation curve, 6 nmol/cm² is needed to saturate the total surface area with $Y(Pr_2amd)_3$. The thickness/cycle saturates at 0.8 Å/cycle;

(23) Hausmann, D.; de Rouffignac, P.; Smith, A.; Gordon, R.; Monsma, D. *Thin Solid Films* **2003**, *443*, 1.

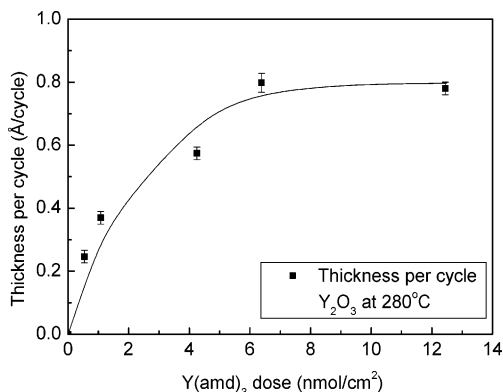


Figure 2. Saturation curve for the Y_2O_3 ALD process using $Y(\text{Pr}_2\text{amd})_3$ and H_2O .

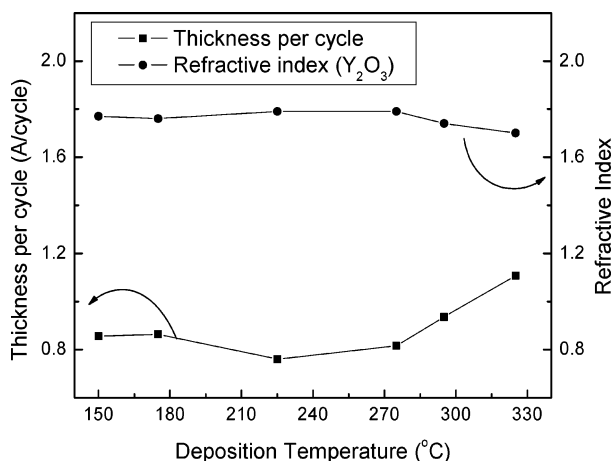


Figure 3. Thickness per cycle and refractive index depend on the deposition temperature.

however, this growth rate is dependent on a sufficiently long purge time in order to fully remove all adsorbed hydroxyl groups ($-OH$) in the bulk of the film. It is known that Y_2O_3 can form a hydroxide or hydrated oxide.²⁴ During the water pulse of the ALD cycle, the ligands are cleaved from the yttrium precursor, but in the process some water is adsorbed by the film. Over a short, but not insignificant, time period the $-OH$ groups are desorbed from the film in the form of water. This desorption produces a water-rich ambient above the film until the excess hydroxyl impurities are fully desorbed and the water has been purged from the reactor. Without sufficient time for this process to finish a localized CVD effect will occur when the subsequent pulse of yttrium precursor is delivered. This effect may explain the higher growth rates seen from the reaction of the $[CH_3Cp]_3Y$ and $[Cp]_3Y$ with water in ref 21. It may also explain the difference in electrical properties seen for the Y_2O_3 films made with the two different precursors.

The growth rate and refractive index were investigated as the deposition temperature was varied from 150 to 330 °C shown in Figure 3. A constant growth rate of 0.8 Å/cycle was maintained from 150 to 280 °C but the growth rate increased rapidly over 280 °C. This rise in growth rate is most likely due to thermal decomposition of the yttrium precursor. The refractive index, which remains constant from 150 to 280 °C, also decreases at higher temperatures.

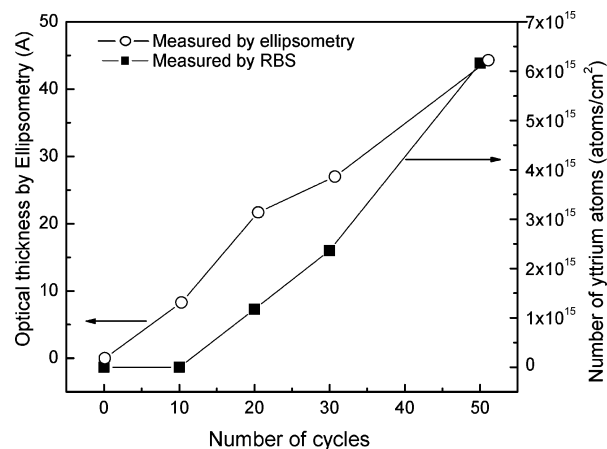


Figure 4. Thickness of Y_2O_3 films grown at 280 °C as a function of the number of deposition cycles.

Thermal decomposition of the yttrium precursor may leave carbon and nitrogen impurities in the film, which would also lead to a higher growth rate and lower refractive index.

Thickness of Y_2O_3 films as a function of the number of deposition cycles is shown in Figure 4. As the number of deposition cycles increases, the thickness of Y_2O_3 films increases linearly with a constant growth rate. This aspect of ALD can provide thickness control on the subnanometer scale. Digital thickness control is important for potential application such as dielectrics in transistors or memories, optical coatings, and in the development of nanotechnology. Digital thickness control also provides a unique opportunity to control the stoichiometry of multicomponent materials such as the superconducting material, yttrium barium copper oxide. Generally, the precursor should be reactive to the starting surface for uniform thin film deposition. To investigate the reactivity of Y_2O_3 to the starting surface, optical (ellipsometry) and physical (RBS) measurements were used to monitor the growth on HF etched silicon. As shown in Figure 4, the optical thickness is around 8 Å after 10 cycles; however, according to RBS, there are no yttrium atoms on the surface. The film seen by ellipsometry may be SiO_2 formed during the initial 10 cycles. It has been reported that in the presence of a metal precursor, Si may be more easily oxidized by H_2O .²⁵ This mechanism supports the idea that an interfacial oxide is growing in during the initial cycles. After 10 more cycles, RBS shows yttrium atoms on Si and the number of yttrium atoms begins to increase linearly with the number of deposition cycles. The inhibition of this Y_2O_3 ALD process is therefore approximately 10 cycles on an HF-last treated surface. It is in good accordance with our $PrAlO_3$ ALD²⁶ process on Si, which has a growth inhibition of 9 cycles.

Another way to test whether reactions are self-limiting is to deposit film on a structure with narrow holes. One such

(25) Harris, H.; Choi, K.; Biswas, N.; Chary, I.; Xie, L.; Mehta, N.; Kipshidze, G.; White, M.; Temkin, H.; Gangopadhyay, S. *Physics and Technology of High-k Gate Dielectrics II*; Proceedings of the Second International Symposium on High Dielectric Constant Materials; Electrochemical Society: Pennington, NJ, 2004.

(26) Rahtu, A.; de Rouffignac, P.; Gordon, R. Lanthanum Aluminum Oxide and Praseodymium Aluminum Oxide [abstract]. In *Atomic Layer Deposition (ALD) of High-K Dielectrics*; Materials Research Society: Warrendale, PA, 2005; Vol 811.

(24) Seitz, A. Z. *Naturforsch.* **1946**, *1*, 321.

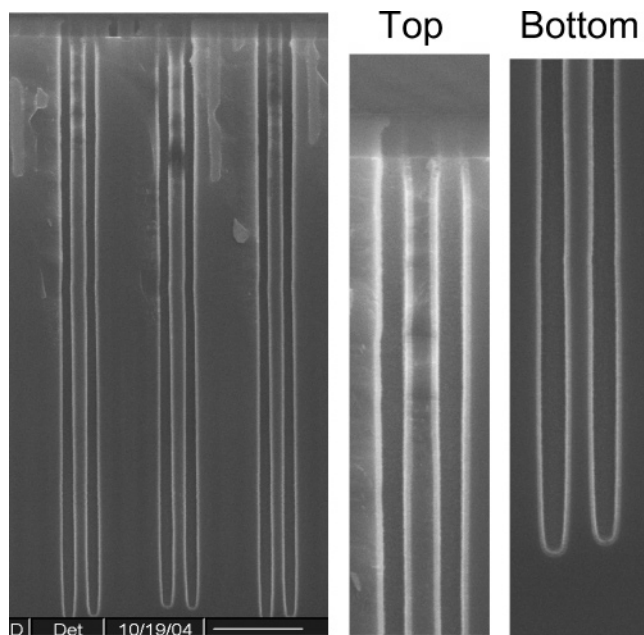


Figure 5. SEM of a 40:1 aspect ratio coated with ~ 280 Å of Y_2O_3 . The scale bar at the bottom right is $1 \mu m$ long. The two images to the right show a magnification of the top and bottom of the center holes in the original scan. Variability from top to bottom is $<5\%$.

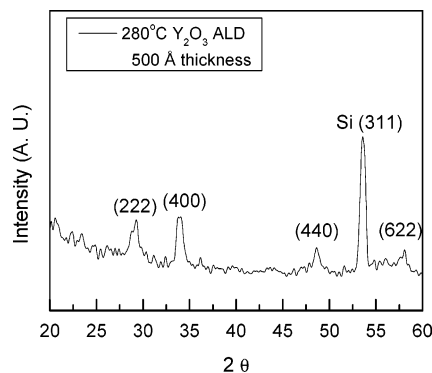


Figure 6. XRD spectrum of a 500 Å thick Y_2O_3 film deposited at 280 °C on silicon. Film is cubic polycrystalline as-deposited.

geometry is found in trench-based DRAMs. These devices incorporate high aspect ratio holes that are coated in a high- k dielectric to form a metal–insulator–metal capacitor with a very high capacitance and a small footprint on the silicon. Using $Y(iPr_2amd)_3$ and H_2O , we found uniform coatings inside holes with aspect ratios in excess of 40:1. Figure 5 shows a 280 Å Y_2O_3 film deposited from 300 cycles of the precursor and water in 40:1 holes. It is impossible to achieve this level of conformality with an ALD process if it involves any decomposition or CVD component.

Film Characterization. The crystallinity of an Y_2O_3 thin film deposited at 280 °C on silicon was determined by XRD. As shown in Figure 6, the film is the cubic polycrystalline phase of Y_2O_3 indicated by the reflections of the (222), (400), (440), and (622) planes. Previous results showed an amorphous Y_2O_3 structure on silicon even at 350 °C using a plasma chemical vapor deposition method,^{27,28} but the ALD

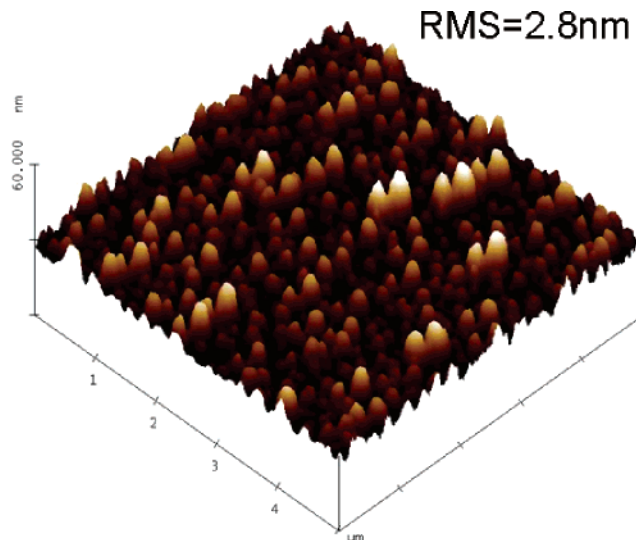


Figure 7. AFM scan of an area $5 \mu m \times 5 \mu m$. Film thickness is 500 Å.

process with ozone as an oxygen source formed crystalline Y_2O_3 .²⁰ Though the other processes require high-energy oxygen radicals to achieve reactivity with those respective precursors, in our case, this new yttrium precursor is very reactive with water and the resulting Y_2O_3 thin films can be formed easily at low deposition temperatures. It may be that this high reactivity allows the film to adopt the lower-energy polycrystalline phase more easily, hence the as-deposited crystallinity.

The surface morphology of the deposited film was analyzed by AFM. An HF treated silicon surface was measured as a reference. The roughness of the bare silicon surface was 3.3 Å. A 2-D root-mean-square (RMS) measurement of roughness was performed on a 500 Å Y_2O_3 thin film deposited at 280 °C and was found to be 28 Å as shown in Figure 7. It was rougher than other plasma chemical vapor depositions, but similar to ALD with ozone. Amorphous ALD thin films (such as Al_2O_3 , $LaAlO_3$, or Ta_2O_5) are usually very smooth films which have an RMS roughness of less than 1% of film thickness, but ALD HfO_2 and ZrO_2 films are rough because they have started to crystallize even at a low deposition temperature.²⁹ Another source of roughness aside from crystallinity is the growth mechanism. Island growth can lead to rough films,³⁰ whereas uniform surface nucleation produces smooth films if they are amorphous. Because of the uniform nucleation of $Y(iPr_2amd)_3$ on Si it can be concluded that the polycrystalline nature of the as-deposited film causes the surface roughness.

RBS (Figure 8) was used to determine the composition of Y_2O_3 films deposited on carbon and silicon at 270 °C. Carbon and nitrogen were found to be less than the detectable limit, <0.5 at. %. This low impurity content can be attributed to both a clean reaction between the water and the $Y(iPr_2amd)_3$ and the lack of thermal decomposition of the precursor. However, the ratio of oxygen to yttrium on the carbon substrate was around 2.0 by RBS, or about 33% higher than expected. The films show a higher ratio of oxygen to yttrium though the new precursor contains yttrium in a +3 oxidation

(27) Durand, C.; Dubourdiou, C.; Vallee, C.; Loup, V.; Bonvalot, M.; Joubert, O.; Roussel, H.; Renault, O. *J. Appl. Phys.* **2004**, *96*, 1719.
 (28) Niu, D.; Ashcraft, R. W.; Chen, Z.; Stemmer, S.; Parsons, G. N. *J. Electrochem. Soc.* **2003**, *150*, F102.

(29) Hausmann, D. M.; Gordon, R. G. *J. Cryst. Growth* **2003**, *249*, 251.
 (30) Puurunen, P. L.; Vandervorst, W. *J. Appl. Phys.* **2004**, *96*, 12.

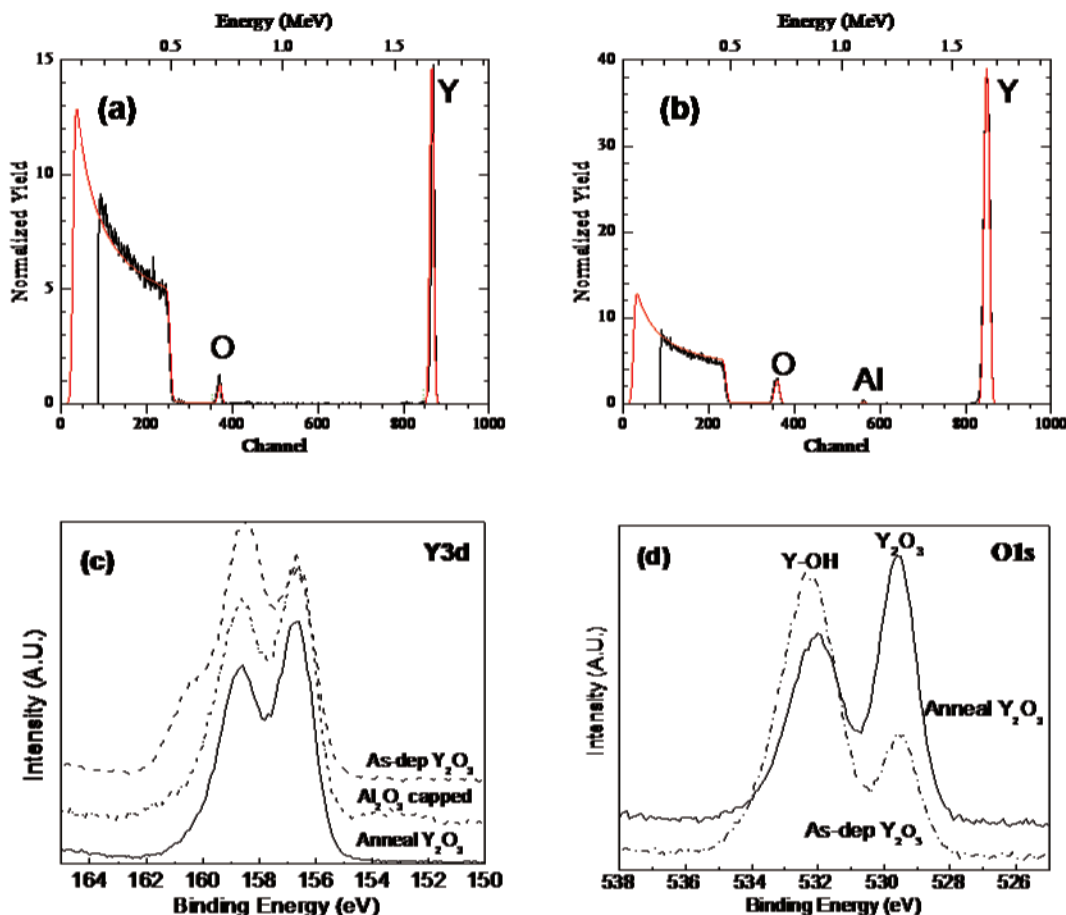


Figure 8. As-deposited films grown at 280 °C: (a) RBS spectrum for as-deposited Y_2O_3 ; (b) RBS spectrum for as-deposited Y_2O_3 with a 10 Å Al_2O_3 capping layer; (c) XPS spectra of Y_{3d} peaks for as-deposited Y_2O_3 , as-deposited Y_2O_3 with Al_2O_3 capping (10 Å), and Y_2O_3 annealed at 400 °C; and (d) O_{1s} peaks for as-deposited Y_2O_3 and Y_2O_3 annealed at 400 °C.

state. As mentioned earlier, water adsorption and incomplete desorption can be a problem for ALD Y_2O_3 films synthesized with water as the oxidant. This phenomenon can also occur slowly when the films are exposed to the ambient atmosphere.³¹ To confirm this as a source of the excess oxygen in the film, ALD Al_2O_3 films were deposited in situ as a capping layer for the as-deposited Y_2O_3 thin films. The capping layer was made up of 10 cycles (~ 10 Å) of Al_2O_3 deposited from trimethylaluminum (TMA) and water at 270 °C. In this case, the ratio of oxygen to yttrium decreased from 2.0 to 1.7. Al_2O_3 as a capping layer can block the adsorption of water from the atmosphere effectively and can help to maintain the purity of Y_2O_3 .

XPS also supports the idea that $-\text{OH}$ groups can be adsorbed by Y_2O_3 . The bonding environment of two films is shown in Figure 8. The Y_{3d} and O_{1s} spectra for an as-deposited, aluminum oxide capped, and an annealed (400 °C for 1 h in Ar) Y_2O_3 film are shown. It has been reported that the $\text{Y}_{3d_{5/2-3/2}}$ doublet position is at 156.7 and 158.7 eV and the O_{1s} peak lies at 529.5 eV for Y_2O_3 .³ In the Y_{3d} case, the as-deposited Y_2O_3 film had a different spectrum from the annealed and Al_2O_3 capped films. As-deposited Y_2O_3 films showed two different bonding pairs, one for pure Y_2O_3 ($\text{Y}_{3d_{5/2}}$, 156.7 eV; and $\text{Y}_{3d_{3/2}}$, 158.7 eV) and one for

the $\text{Y}-\text{OH}$ bond (Y_{3d_5} , 158.8 eV; and $\text{Y}_{3d_{3/2}}$, 160.6 eV).³² The $\text{Y}_{3d_{3/2}}$ peak in the as-deposited film was higher in intensity than the $\text{Y}_{3d_{5/2}}$ peak even though the $\text{Y}_{3d_{5/2}}$ peak in a normal Y_2O_3 spectrum should be higher in intensity than the $\text{Y}_{3d_{3/2}}$ peak. It suggests that another phase of Y_2O_3 gives rise to the peak at 158.7 eV. The shoulder seen for the as-deposited film at 160.5 eV matches the peak expected for $\text{Y}-\text{OH}$. In addition, the O_{1s} spectrum shows that two different oxygen bonding states exist in the as-deposited films. O_{1s} peaks were located at 529.5 and 532.0 eV. The lower-energy O_{1s} peak is very consistent with the normal $\text{Y}-\text{O}$ bonding energy in Y_2O_3 . There are several possibilities for the identity of the higher energy peak. As reported in the literature, $\text{Y}-\text{O}-\text{C}$ types of bonds such as $\text{C}=\text{O}$ can be picked up from surface contamination or incorporated into the film from the precursor; however, the bond energy of $\text{C}=\text{O}$ is slightly lower than what was seen for this film.³ In some cases an interfacial oxide or silicate could cause this peak, but the film was thicker than the penetration depth of the XPS system and there were no Si related peaks that could be detected. The higher-energy O_{1s} peak most likely corresponds to hydroxyl groups bound to yttrium atoms.

The Y_{3d} spectra for the annealed film and the Y_2O_3 film with an Al_2O_3 capping layer did not have a shoulder or different peak intensity compared to the accepted spectrum

(31) Niu, D.; Ashcraft, R. W.; Parsons, G. N. *Appl. Phys. Lett.* **2002**, *80*, 3575.

(32) Ulrich, M. D.; Rowe, J. E.; Niu, D.; Parsons, G. N. *J. Vac. Sci. Technol. B* **2003**, *21*, 1792.

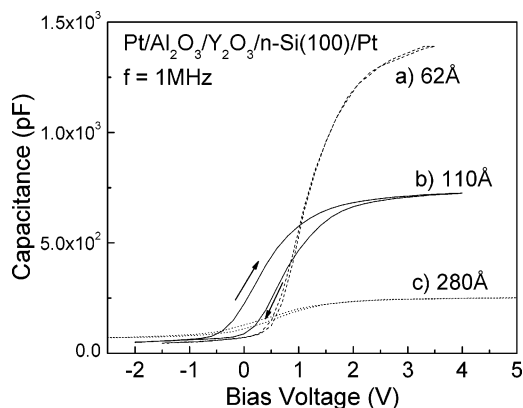


Figure 9. Capacitance–voltage curves of Al_2O_3 (10 Å thickness except for (a) 5 Å) capped Y_2O_3 films. The labels indicate the physical thickness.

of Y_2O_3 . But the O1s spectrum is more sensitive to the presence of Y–O–OH bonding and it shows a small peak for the annealed film, but not the capped film. Exposure of the sample to air can lead to rapid water adsorption on the surface if the film is not capped.

Electrical Properties. The capacitance–voltage (CV) curves of Y_2O_3 films are shown in Figure 9. Y_2O_3 thin films were deposited at 280 °C on HF etched n-type silicon, followed by an in-situ deposition of a ~ 10 Å Al_2O_3 thin film. The Al_2O_3 film was grown by ALD using 10 cycles of TMA and water at the same deposition temperature. Capping of the Y_2O_3 films helps prevent adsorption of water after air exposure. Platinum dots with an area of 1.05×10^{-3} cm² were sputtered on through a shadow mask. For a film (a) the equivalent silicon oxide thickness (EOT) was calculated by Hauser’s CVC program³³ to be 2.25 nm with a flat band voltage (V_{FB}) of 1.1 V, and low hysteresis (27 mV). In the case of the 110 Å thick Y_2O_3 film (EOT ≈ 37 Å), the permittivity and average flat band voltage are 11.4 and 0.61 V, respectively. As the film thickness increased to 280 Å (EOT ≈ 87 Å), the CV curve stretches out. It might be from increasing charge traps in the films.³⁴ These traps could come from the increase in –OH content that would occur as the film thickness increases. The Al_2O_3 capping layer prevents water from penetrating from the atmosphere, but there may be –OH groups remaining from the deposition itself. The dielectric constant is around 12 for films (b) and (c), but drops to 11 for film (a). Though the variation is small it is possible that there is an interfacial layer that consists of SiO_2 or a mixed silicate which lowers the overall permittivity of the insulating layer. When corrected for a 1-nm SiO_2 interfacial layer the dielectric constant of (a) is also 12.

Current density as a function of electric field (J – E) was measured to determine the leakage current and dielectric breakdown of several Y_2O_3 films as shown in Figure 10. In Figure 10, Y_2O_3 films were deposited with the same thickness (~ 300 Å) under different deposition temperatures (270, 280, and 295 °C). All films showed a high breakdown field near

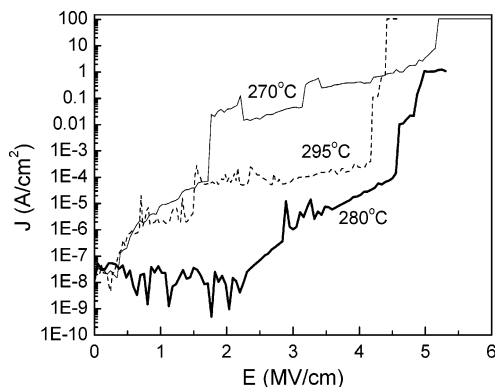


Figure 10. Current density as a function of electrical field for three Y_2O_3 films deposited at three different temperatures (270, 280, 295 °C). All films deposited on HF-last Si and are 30 nm thick.

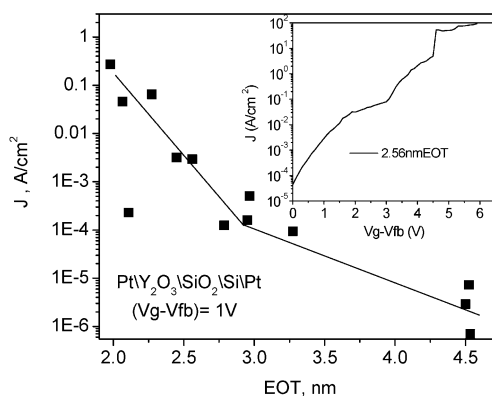


Figure 11. J vs E_{OT} at a gate voltage of 1 V (compensated for V_{FB}) with J vs V_G for the 2.56 nm EOT film inset.

4–5 MV/cm which satisfies a requirements for advanced CMOS (complementary metal oxide semiconductor) gate oxide specifications. In the case of the Y_2O_3 deposited at 280 °C, the leakage current level was below 10^{-7} A/cm² even at 2.5 MV/cm. The Y_2O_3 films deposited at other temperatures (270 and 295 °C) showed 10^{-6} A/cm² at 1 MV/cm and were leakier than those deposited at 280 °C. As mentioned before, thermal decomposition of the yttrium precursor can result in the incorporation of carbon impurities in films over 280 °C and residual carbon impurity can lead to comparably leaky Y_2O_3 films. In addition, negative charges such as –OH groups might explain the higher leakage current density seen in the Y_2O_3 films deposited below 270 °C. Purging times become quite long at the lower temperatures if they are to be fully desorbed of water. To expand the zone of adequate electrical properties it would be necessary to increase the purge times to remove excess water, or to design a modified precursor that is more thermally stable.

Figure 11 shows a plot that uses leakage current density values obtained at 1 V, where the voltage is compensated by the flat band voltage. This plot shows the amount of current leakage through the gate oxide while the MOSFET is in the on state. The inset shows the J vs ($V_G - V_{FB}$) curve for the lowest E_{OT} film. This level of leakage is the lowest reported in the literature by any CVD or ALD method for ultrathin Y_2O_3 thin films. The average breakdown field of 5 MV/cm is also the highest breakdown field reported thus far.^{17–21}

(33) Hauser, J. R.; Ahmed, K. In *Characterization and Metrology for ULSI Technology*; Seiler, D., G., Ed.; American Institute of Physics, Woodbury, NY, 1998; pp 235–239.

(34) Choi, K.-J.; Shin, W.-C.; Yoon, S.-J. *J. Electrochem. Soc.* **2002**, *149*, F18.

Conclusions

Yttrium oxide thin films were successfully deposited by ALD with a new precursor, yttrium tris(*N,N'*-diisopropylacetamidate), $\text{Y}(\text{Pr}_2\text{amd})_3$, and water over a wide temperature range (150–280 °C). Water acted as the oxygen source and cleanly removed the ligands from the precursor to make Y_2O_3 films. The yttrium precursor was suitable for depositing pure Y_2O_3 films because it was thermally stable, volatile (30 mTorr at 90 °C), and had good reactivity with water. Y_2O_3 ALD films grew at a rate of 0.8 Å/cycle and had a refractive index of ~ 1.8 . The films were smooth and had a cubic polycrystalline structure. The structure was also shown to be permeable to water both during the deposition and when

exposed to air. An in situ deposition of an Al_2O_3 capping layer helped to prevent water adsorption after exposure to air; however, the film still retained a small but detectable number of –OH groups. The as-deposited Y_2O_3 films exhibit a high dielectric breakdown field (5 MV/cm), a relatively high permittivity (~ 12), and a low-leakage current density ($< 10^{-7}$ A/cm² at 2.5 MV/cm) at 280 °C.

Acknowledgment. We thank Infineon for samples of the DRAM trenches. This work was supported in part by the National Science Foundation.

CM050624+